Energy Reports 8 (2022) 11569–11578

Contents lists available at ScienceDirect

Energy Reports

journal homepage: www.elsevier.com/locate/egyr

Research paper

A stochastic model for estimating electric vehicle arrival at multi-charger forecourts

F.M. Aboshady [a], I. Pisica [a,c], C.J. Axon [b,c,*]

[a] Department of Electronic and Electrical Engineering, Brunel University London, Uxbridge, London, UK
[b] Department of Mechanical and Aerospace Engineering, Brunel University London, Uxbridge, London, UK
[c] Institute of Energy Futures, Brunel University London, Uxbridge, London, UK

ARTICLE INFO

Article history:
Received 5 June 2022
Received in revised form 24 August 2022
Accepted 4 September 2022
Available online xxxx

Keywords:
Charging station
Driving behaviour
Electric vehicle
EV charging
EV power demand
Rapid charging

ABSTRACT

Many countries are observing significant growth rates in electric vehicle (EV) uptake, often backed by financial incentives or regulation and legislation. The availability of large multi-charger sites for rapid EV charging with an experience similar to conventional refuelling stations lowers the barrier to acceptance for drivers considering the switch to using an EV. The question arises about how to size such a facility at the design and planning stage, as well as accommodating growth in the number of EVs in daily use. One of the important factors is the vehicle arrival rate and the corresponding power and energy demand. EV charging is a function of several parameters, all of which are stochastic in nature, such as the vehicle daily travelled distance, charging start time and the required energy. To account for uncertainty in the parameters, a stochastic model has been designed to simulate realistic vehicle arrival rates. The model accounts for EVs coming from the site catchment area and opportunistic charging from passing traffic travelling on the major roads adjacent to the site, the seasonality of parameters, and charging at places other than the site (competitive charging). The model produced plausible EV arrival patterns for both local and passing traffic, and reproduced the characteristic power demand at the case study site. All estimates incorporate uncertainty, reflecting realistic variability of the important parameters. The model in independent of location, uses open-source data, and is structured flexibly, making it adaptable to new sites as part of the technical and business planning process.

1. Introduction

The aim of electrifying transport is to reduce greenhouse gas (GHG) emissions. In the UK the anticipated reduction in the carbon dioxide emissions is between 50% and 87% by 2050 compared to 2014 due to EV uptake, improved efficiency of internal combustion engine vehicles and decarbonization of the electricity supply (Hill et al., 2019; Bharathidasan et al., 2022). Interest in trialing EVs and charging infrastructure is worldwide, for example: China (Zheng et al., 2020), Finland (Uimonen and Lehtonen, 2020), Ireland (Morrissey et al., 2016), New Zealand (Su et al., 2019), South Korea (Moon et al., 2018), UK (Robinson et al., 2013), and USA (Harris and Webber, 2014; Tehrani and Wang, 2015; Almutairi and Alyami, 2021). Barriers to the spread of EVs include limited availability of charging infrastructure, low charging power (long EV recharge time) and limited electrical range (Elghitani and El-Saadany, 2021; Goel et al., 2021). Most frequently charging infrastructure has been limited to individual home charging, *adhoc* on-street charging, and small collections of chargers at workplaces. For the normalization of EV use, charging needs to be more convenient, and it is proposed that an experience similar to current refuelling stations will be required i.e. public sites with many chargers available. However, this has attendant issues such as estimating the likely vehicle throughput and the impact on the local distribution grid (estimating the maximum instantaneous power demand). Neither of these issues are deterministic, but must be simulated stochastically.

Although EVs reduce tailpipe emissions, they introduce a new type of electric load (Birk Jones et al., 2022; Ahmad et al., 2022). It is widely recognized that grid constraints are an obstacle to greater EV uptake (Qian et al., 2011; Steen et al., 2012; Robinson et al., 2013; Harris and Webber, 2014; Morrissey et al., 2016; Su et al., 2019; Cheng et al., 2022). The majority of studies consider the effects of home charging (Qian et al., 2011; Harris and Webber, 2014; Tehrani and Wang, 2015; Brady and O'Mahony, 2016; Morrissey et al., 2016; Ul-Haq et al., 2018; Su et al., 2019; Almutairi and Alyami, 2021). Work place (Brady and O'Mahony, 2016; Uimonen and Lehtonen, 2020) and public (Qian et al., 2011; Morrissey et al., 2016) charging have also been considered. Most EV charging uses uncoordinated low to medium power charging

* Corresponding author at: Department of Mechanical and Aerospace Engineering, Brunel University London, Uxbridge, London, UK.
E-mail address: Colin.Axon@brunel.ac.uk (C.J. Axon).

https://doi.org/10.1016/j.egyr.2022.09.007

points at home, work, and public places. Currently 81.4% of UK public installed charging points have power ratings $\leq$22 kW and only 3.9% are $\geq$100 kW (Zap-MAP, 2021). Home charging is limited to 3–5 kW requiring off-street parking often unavailable to those living in apartments or other high-density housing. Dedicated high-speed charging stations will allow drivers to charge without needing to arrive at their destination (Dixon et al., 2018).

The load profile of an EV is determined by several stochastic factors such as the daily travelled distance and the battery state-of-charge (SoC) at start of the day (Humayd and Bhattacharya, 2018). Deterministic modelling is not a suitable mean to estimate the EV load profile as it does not reflect the stochastic nature of the important variables, but non-deterministic approaches have not received sufficient attention (Buzna et al., 2021). Zhang et al. (2020) divide EV infrastructure modelling into computational geometry and origin–destination flow-based approaches. Different models have been reported to forecast/estimate the aggregated EVs load profile (Shepero et al., 2018; Daina et al., 2017). Modelling methods use a variety of statistical and probabilistic techniques (Tehrani and Wang, 2015; Brady and O'Mahony, 2016; Uimonen and Lehtonen, 2020; Zheng et al., 2020), agent-based models (Zhang et al., 2020), Gaussian mixture models (Powell et al., 2022), Monte Carlo simulation (Harris and Webber, 2014; Almutairi and Alyami, 2021; Sadhukhan et al., 2021), Markov chain (Ul-Haq et al., 2018; Yan et al., 2022), ensemble methods (Buzna et al., 2021), and deep learning (Zhu et al., 2019a,b). Most studies use travel data and vehicle specifications, but demographic data (Steen et al., 2012), building occupancy (Uimonen and Lehtonen, 2020), and user preference (Robinson et al., 2013; Moon et al., 2018) have also been used. Probability distribution functions have been used (Almutairi and Alyami, 2021) to represent variables such as the EV home arrival time, home departure time and daily mileage. The daily load profile was estimated for each EV and accumulated for all vehicles resulting in the total fleet load profile. The copula method has been used (Tehrani and Wang, 2015) to develop set of random variables with joint probability distributions.

In assuming that EVs charge at end of each trip to generate probability distributions throughout the day and giving different probabilities of charging to plug-in hybrid electric vehicles (PHEVs) and the battery electric vehicles (BEVs), Harris and Webber (Harris and Webber, 2014) used Monte Carlo simulations to estimate the load demand. In Brady and O'Mahony (2016), the dependence structure between the first departure time in the day, number of journeys per day and total distance travelled was modelled using a non-parametric copula function. Then, a travel pattern was generated considering uncertainty of the inputs. Upon arrival at a destination, a probabilistic charging decision model calculates the probability of charging given the EV battery state of charge, the available parking time and the current journey number. The model depends on using slow home/work chargers and assumed that it is more likely an EV charges after the first or second journey due to arriving at work.

Attention has been paid to characterizing charging demand using surveys and by analysing recorded charging events. A Korean survey (Moon et al., 2018) estimated the increase in the electrical load due to the expansion of EVs and its affect on the electric grid. The survey included questions about EV users' preferences such as time of the day, location and type of charging point used to recharge the EVs. This showed that the users prefer to use fast public charging points during the peak hours of the day while charging at home during the night. Fast charging points are preferred by users of the public chargers which will be commercially available in the short to medium term (Morrissey et al., 2016). A study of charging habits in the north east of the UK combined both private and organizational users (Robinson et al., 2013). Analysis of 7704 charging events showed that private users peak demand was at the evening when the drivers arrive home (home charging) while the organizational drivers primarily charge their EVs at the work. Charging events at a wide variety of locations and types of chargers in the San Francisco area have been analysed and modelled to estimate charging demand (Powell et al., 2022).

Unscheduled EV charging places stress on the electric grid (Harris and Webber, 2014). In Zhu et al. (2019b,a), different deep learning approaches have been used and compared for short-term load forecasting of EV charging. Real charging events recorded in Shenzhen, China, have been used for the training and testing of the models. By segmenting the fleet (Zheng et al., 2020) studied mid-and-long term load forecasting using a probabilistic approach incorporating market evolution, giving projections of future EV ownership. To enhance the power system operation and to help setting the network reinforcement or upgrade plans, stochastic modelling for EV load demand was proposed (Qian et al., 2011). Comparison between four charging scenarios (Qian et al., 2011): (1) uncontrolled domestic charging, (2) uncontrolled off-peak domestic charging, (3) smart domestic charging and (4) uncontrolled public charging, showed that the uncontrolled domestic charging causes the highest increase in the system peak load. The model assumed that private EVs charge once every two days while company EVs charge once per day.

Two models estimate loads for fast-charging stations in a stochastic manner: a station with six 50 kW chargers (Deng et al., 2018) and 50 stations each with one 50 kW charging point (Korolko et al., 2016) (defaults to home-charging with a 10% station-use probability). The fleet size was defined according to the national average size of EVs per installed charger (with uniform distribution). Moradipari et al. (2021) studied how to influence where EV users charge to reduce both the aggregate congestion at fast-charging points installed at different locations and impact on the electric grid. An energy management approach (Huo et al., 2017) forecasts charging demand assuming a Poisson process where EVs start with 10%–40% SoC, terminating at 80%. For a 3-charger station 100 EVs were assumed to arrive every day. Google Maps Popular Times data for all petrol stations in the UK was used in a Monte Carlo model to estimate the EV arrival at a fast-charging station (Dixon et al., 2018). Probability distributions were assigned to EV initial and final SoC while converting the arrival rate to a demand profile. Most models do not consider location-dependent factors/parameters, instead using an average station occupancy.

Most previous models rely on finding the periods of time EVs are at home/work/public place, then checking the charging probability during these intervals. Others concerned about fast charging estimate an average occupancy of the charging connection or study the aggregate influence of dispersed charging points on the electric grid. Typically, studies have been concerned with power demand from EVs at a highly aggregated system level e.g. Tang and Wang (2016), Yi and Bauer (2016), Zhang et al. (2020), Kavianipour et al. (2021) and Pan et al. (2020) and are focused on infrastructure planning for a geographic area or region. The charging requirements of EVs has been incorporated into a stochastic transport model as part of a smart city simulation (Duan et al., 2021).

In this paper, EV arrival at a multi-charger electric forecourt is treated like conventional (liquid) refuelling stations, which is expected to be the preferred method in a mature EV market. To the authors best knowledge, work reported in the literature regarding EV charging demand allocation/estimation lacks a detailed study concerning a dedicated multi-charger forecourt with EVs charging during a journey. The aim of this paper is to model EV arrival rates and power demand for a dedicated charging station. The model

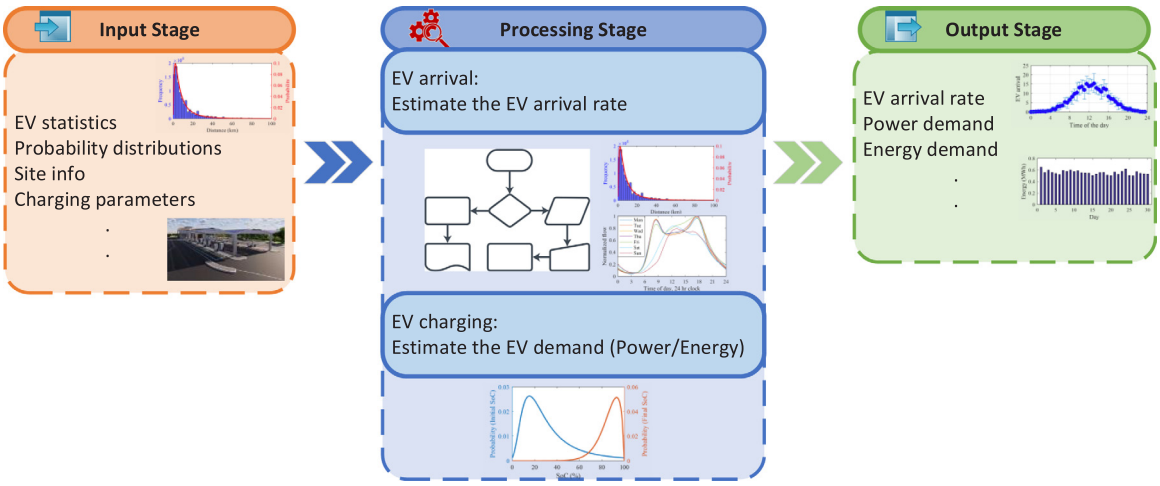

Fig. 1. Structure of the proposed model.

helps optimize the forecourt operation by using parameters specific to the forecourt location, such as registered BEV/PHEVs by zipcode and real-world traffic flow on nearby roads, to forecast the EVs arrival rate and the corresponding power/energy demand. Moreover, the model has the following features which are not fully incorporated in a single model in the literature:

1. A stochastic approach incorporating uncertainty in the parameters controlling the charging process.
2. Considers probabilistic EV charging from both residents and travelling EVs (different populations).
3. PHEVs and BEVs are treated independently with different probabilities.
4. Real-world sale statistics are used to derive information about the EV market share and fleet composition in different populations instead of assuming a national average EV distribution.
5. Accounts for seasonality in the parameters.
6. Considers charging at other places other than the electric forecourt (competitive charging).

The approach is to use real-world open-source data to ensure that the method is widely applicable. For validation, a convenient case-study is the UK's first dedicated multi-charger station, located at Braintree in Essex County. It is an integrated, utility-scale site consisting of 24 ultra-rapid DC chargers (of various power ratings from 90 kW to 350 kW) with charging times of less than 30 min, plus 6 AC chargers (up to 22 kW) and 6 T superchargers. This facility may mitigate the burden on the local distribution system the as the site is connected to the 33 kV grid. The model will help predict likely near-term site use, understand patterns of use to assist in developing similar sites, optimize revenue, and maintain assets.

2. Model design

The model is developed from an outline given in Aboshady et al. (2021), to include seasonality, competitive charging with facilities beyond the site, and charging EVs from adjacent geographical districts. The structure of the proposed model is shown in Fig. 1 has three stages. Different input parameters are fed to the model in the first stage. The processing stage estimates the arrival rate and the corresponding load demand. Lastly, the model outputs the variables of interest.

For any day, the need to charge depends on parameters such as daily travelled distance and the battery state of charge (SoC) at the start of the day. Most of the parameters are probabilistic in nature. Therefore, a stochastic approach of EV arrival accounts for the uncertainty observable in real-world data. The arrival model first estimates the number of EVs arriving at the site at each of 48 half-hour slots (aligning with the National Grid settlement period). Then, we estimate the power and energy demand for these EVs.

The model uses two population-based estimations namely EV owners living or working nearby, and traffic passing along the main roads surrounding the site. For instance, an EV driver may plan to use the site for recharging during a long journey. Each population has different charging requirements and is modelled independently. For modelling different parameters, data from the literature is used.

2.1. The local population of EVs

The local fleet combines EVs in the adjacent areas plus 25% (assumed) of the next-nearest areas, concentric to the site. Regarding the Braintree site used as a case-study, this gives 406 BEVs and 303 PHEVs registered at the end of 2020 (Department for Transport, 2020b). Their behaviour is tied to the daily travelled distance.

Modelling EV arrival rate for the local population has two steps. Firstly, the number of EVs (N_{ev}) most likely needing to charge in the next 24 h is estimated. The second step uses the output of the first to estimate the number of EVs for each of the 48 half-hour periods. Each EV's SoC is related to the total distance travelled since the last charging event. Assuming the SoC decreases linearly with the distance travelled, the likely current SoC is calculated by

$$SoC_c = SoC_f - (d/D)\times 100\% \quad (1)$$

where SoC_c and SoC_f are the current and final SoC respectively, and d and D are the total travelled distance (accumulated daily travelled distance since the last charging event) and total electrical range for the EV, respectively. The total electrical range, battery capacity, and charging rate depend on the EV model (EV Database, 2020). A database with the common EV models and their market share is constructed. From this database, an EV model is picked randomly, based on their relative market share, for each EV in the local fleet (Department for Transport, 2020b). The distribution modelling the uncertainty in the daily travelled distance is derived from the UK National Travel Survey (Department for Transport, 2017). The data (Fig. 2) is fitted to

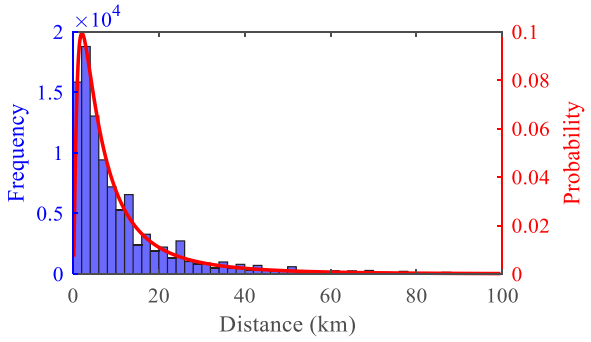

Fig. 2. Histogram of daily travelled distance (blue) and modelled distribution (red line).
Source: Department for Transport (2017).

Table 1
Plug-in time distribution parameters.

Postcode	Winter	Spring	Summer	Autumn
Mean	14:00	13:12	13:24	13:42
Standard deviation	3 h 42 min	4 h 6 min	4 h 2 min	4 h 12 min

a lognormal distribution (2). The mean and standard deviation coefficients for the distribution are 1.9 and 1.1, respectively.

$$f\,(d|\mu,\sigma) = \frac{1}{d\sigma\sqrt{2\pi}}\exp(-\frac{(\ln d-\mu)^2}{2\sigma^2}) \tag{2}$$

where $f\,(d|\mu,\sigma)$ is the probability density function at distance d, μ is the mean value and σ is the standard deviation.

If the likely SoC_c for an EV is $<$ 20% the EV needs charging in the next 24-h period, giving N_{ev} for the local population. The sequence describing this first step is illustrated by Algorithm I (Appendix). Next, we estimate the EV arrival for the 48 half-hour slots using a plug-in time distribution. Real-world charging events recorded in Essex County in the UK. are used to build the seasonal plug-in time distribution (Department for Transport, 2020a). The data is fitted to a normal distribution (3) with mean and standard deviation given in Table 1,

$$f\,(t|\mu,\sigma) = \frac{1}{\sigma\sqrt{2\pi}}\exp(-\frac{1}{2}\left(\frac{t-\mu}{\sigma}\right)^2) \tag{3}$$

where $f\,(t|\mu,\sigma)$ is the probability density function at t, μ is the mean value and σ is the standard deviation.

For each time slot, the likelihood calculated from the plug-in time distribution is used as a threshold value. A random integer between zero and an upper limit is generated. The upper limit for the first time slot is N_{ev} and is recursively decreased for the remaining time slots to account for the EVs charged during the previous time slots. This integer (N) represents the maximum possible number of EVs arriving at this slot. To decide how many EVs arrive at the current time slot, N random values between 0 and 1 are generated. Each value is compared with the threshold value at this time slot. The EV is counted as a new arrival if the random value is less than or equal to the threshold value. The sequence describing this second step is illustrated by Algorithm II (Appendix).

2.2. Passing traffic population

Arrivals from this population depend on the daily flow on the nearby roads. For this case-study (Braintree site), three major roads are considered, A12, A120 and A131, using the flow on an average day of the year (Department for Transport, 2019). The variance in traffic flow between months of the year can be considered using the relative monthly flow (Department for Transport, 2019) (Table 2). From the average daily vehicle flow, the expected EV flow is estimated using the EV market share. The licenced BEVs and PHEVs in the UK at the end of 2019 are 0.3% and 0.4%, respectively, of the total fleet (Department for Transport, 2020b). Therefore, the total EV share (0.7%) is used to scale the total vehicle flow to represent the passing EV flow. Not all vehicles on the roads are travelling long distances. The National Travel Survey dataset (Department for Transport, 2017) showed that car trips longer than 25 miles are only 7% of the total trips. This is used to distinguish long journeys from the average EV daily traffic flow. Thus, the daily vehicle flow is scaled by two factors to reflect the EV flow travelling long distances.

Table 2
Average daily traffic flow by month, average = 100.

Month	Jan.	Feb.	Mar.	Apr.	May	Jun.	Jul.	Aug.	Sep.	Oct.	Nov.	Dec.
Value	90.4	95.1	98.0	101.2	103.7	104.5	104.6	104.0	103.4	100.9	98.9	95.0

Table 3
Traffic flow distributions parameters.

Gaussian mixture	Value	Generalized extreme	Value
Mean	[17.3, 9.6]	Location	12.7
Covariance	[8.6, 8.4]	Scale	5
Proportion	[0.53, 0.47]	Shape	−0.373

The EV daily flow is distributed throughout the day using the normalized motor vehicle flow distribution by time of the day (Fig. 3) (Department for Transport, 2019). All weekdays show similar distributions with two peaks, and the weekends are similar with a single peak in the afternoon. A Gaussian mixture distribution, comprising multivariate Gaussian distribution components, is used for the weekdays (4). The mean, covariance, and proportion values for the distribution are given in Table 3. A generalized extreme value distribution (5) is used for the weekends with the distribution parameters (Table 3). These distributions are equivalent to the plug-in time distribution required with the local population modelling. Accordingly, each time slot has a maximum possible number of EVs (upper limit). For each time slot, several random values are generated between 0 and 1. The slot upper limit determines how many random values are generated. These values are compared with a threshold level (TF_{thr}). An EV is counted as a new arrival if the generated random value is less than or equal to the threshold level. The influence of the TF_{thr} value is studied later in the competitive charging subsections.

$$\begin{aligned} p\,(t) &= \sum_{i=1}^{n} w_i f\,(t|\mu_i,\sigma_i) \\ f\,(t|\mu_i,\sigma_i) &= \frac{1}{\sigma_i\sqrt{2\pi}}\exp(-\frac{1}{2}\left(\frac{t-\mu_i}{\sigma_i}\right)^2) \\ &\sum_{i=1}^{n} w_i = 1 \end{aligned} \tag{4}$$

where $p\,(t)$ is the probability density function at t for a weekday, μ_i, σ_i and w_i are the mean, the covariance, and the proportion value for the ith distribution and n is the number of distributions. In this case, $n = 2$.

$$\begin{aligned} f\,(t|k,\mu,\sigma) &= \frac{1}{\sigma}Q^{k+1}\exp(-Q) \\ Q &= \left(1+k\frac{t-\mu}{\sigma}\right)^{-\frac{1}{k}} \end{aligned} \tag{5}$$

where $f\,(t|k,\mu,\sigma)$ is the probability density function at t for a weekend, μ, σ and k are the location, the scale, and the shape parameters for the generalized extreme value distribution.

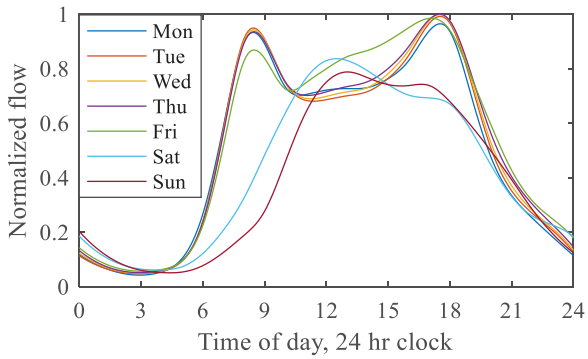

Fig. 3. Traffic flow distribution.
Source: Department for Transport (2019).

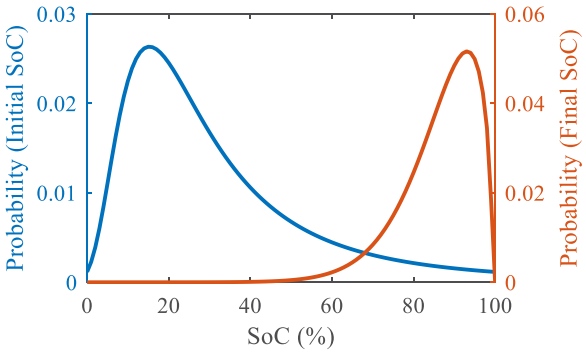

Fig. 4. Initial and final state of charge distributions.

Table 4
Parameters for the initial and final SoC distributions.

Initial SoC	Value	Final SoC	Value
Location	20	Location	85
Scale	15	Scale	10
Shape	0.4	Shape	−0.7

2.3. Competitive charging

As EVs may charge at other locations e.g. home, work, or public standalone charging points, the proposed model includes a competitive charging probability for each population.

2.3.1. Local population competitive charging factor

For each EV from the local population, N_{ev}, a random value between 0 and 1 is generated and compared with the competition factor to decide if that EV is going to be a potential arrival from the local population or is going to charge elsewhere. If the random value is less than or equal to the competition factor, then this EV is counted as a possible new arrival. Otherwise, it is assumed that this EV is going to charge elsewhere. Accordingly, a modified value for N_{ev} is calculated and used as an input to the second step of the local population algorithm. It is expected that the site is mostly used by BEVs rather than PHEVs because of their larger battery capacity, thus benefitting from higher charging rates. Hence, two competition factors are used, BEV_{com} and PHEV_{com}.

2.3.2. Passing traffic population competitive charging factor

The competitive charging is implemented by controlling the threshold level used to determine the new arrivals (TF_{thr}). PHEVs have the option of using the engine, so to account for the lower likelihood of charging, the PHEV market share is scaled down by a factor ($PHEV_{rt}$) when estimating the EV flow. Therefore, the BEV to the PHEV effective ratio participating in the passing traffic increases. The effective EV share in the passing traffic is therefore estimated by (6) with the second term representing the PHEV effective share in the passing traffic,

$$\text{EV share} = \text{BEV share} + PHEV_{rt} \times \text{PHEV share} \tag{6}$$

A study setting the competitive charging parameters is carried out in Section 3.

2.4. EV charging

Thus far, only the EV arrival rate is modelled. This section shows how to estimate the load demand corresponding to the estimated EV arrivals. As previously mentioned, a database for the common EV models is constructed and used to randomly pick the EV model for each new arrival based on the relative EVs share in the market (Department for Transport, 2020b). The EV model defines the rated charging power, battery capacity, and total electrical range. The BEVs and PHEVs in the local population is defined using the relative share of the common models. For the passing traffic population, firstly the EV is chosen to be BEV or PHEV based on their relative share in the population. For example, if the BEV and PHEV relative share is 80% and 20% respectively. A random value is generated between 0 and 1. If the random value is less than or equal to 0.8 then the vehicle is considered a BEV, otherwise, a PHEV. Then a vehicle is selected using the relative share of the common BEVs and PHEVs, similar to the local population case.

The energy demand of an EV is drawn from the combination of initial SoC, final SoC and the EV battery capacity because the energy distribution may be biased based on the EV type. The likely initial SoC is estimated by (1) for the local population. However, it is not predicted for the passing traffic population. Common distributions for the initial SoC (Qian et al., 2011) and final SoC (Schäuble et al., 2017) are used (Fig. 4). Both initial and final SoC distributions are represented by generalized extreme value distribution with the parameters given in Table 4.

The EV charging status time step (Δt) is 2 min. The EV charging power is assumed to be the rated EV value. The charging session ends when the amount of energy charged is equal to the required energy. A 1% probability is assumed that the user terminates the charging session before its planned end. Therefore, the power delivered by each charger and the total power (from all chargers) is recorded with a resolution Δt throughout the day. The total power demand is calculated using (7), where N_{ch} is the total number of chargers in the charging station. This power profile represents the expected load profile for the next day which can be integrated in the optimization process controlling the site operation.

$$P(t) = \sum_{i=1}^{N_{ch}} P_i(t) \tag{7}$$

3. Results and discussion

3.1. Competitive parameters: setting and model sensitivity

A study is performed on the influence of the four parameters controlling the competitive charging namely BEV_{com}, $PHEV_{com}$, TF_{thr}, and $PHEV_{rt}$ on the model output, and to guide setting the values. The total monthly energy required to charge the EVs and the percentage of charging sessions related to charging BEVs

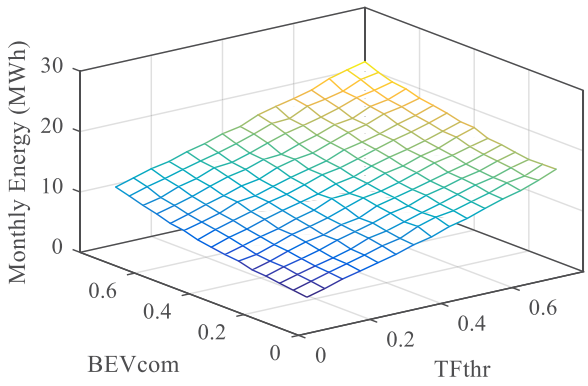

Fig. 5. Variation of BEV_{com}, TF_{thr} with monthly energy demand.

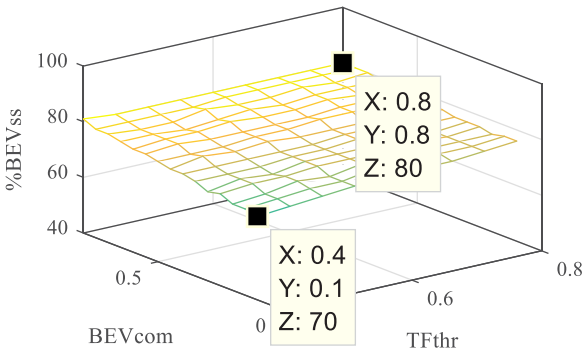

Fig. 6. Variation of BEV_{com}, TF_{thr} with $\%BEV_{ss}$.

($\%BEV_{ss}$) are considered as the outputs of interest when setting the competitive charging parameters. As more charging events are for BEVs, the monthly energy demand is dominated by BEVs rather than PHEVs. So, the BEV_{com} for the local population and the TF_{thr} for the passing traffic population are the important parameters from an energy point of view. The other two parameters ($PHEV_{com}$ and $PHEV_{rt}$) control the $\%BEV_{ss}$ level.

Deep testing is performed to (1) derive the relationship between the parameters and the model output, (2) define the feasible range for each parameter, and (3) provide a guide for setting the parameters. Testing is performed over a wide range of values for the parameters using the following tests. For all cases the model has been executed 15 times for each test point.

3.1.1. BEV_{com}, TF_{thr} and monthly energy

To study the relationship between the BEV_{com}, the TF_{thr}, and the energy demand, each of the BEV_{com} and the TF_{thr} were varied between 0.1 to 0.8 in 0.05 steps while keeping $PHEV_{com}$ and $PHEV_{rt}$ fixed at 0.1 and 0.25, respectively. Fig. 5 shows the average monthly energy. The standard deviation for the 15 model executions at each point has been calculated and the average standard deviation for all points is 0.57 MWh. The following observations can be made from Fig. 5:

- the monthly energy increases with increasing any of the two parameters, and
- both BEV_{com} and TF_{thr} have a close to linear relationship with total monthly energy.

The operational data suggests that the $\%BEV_{ss}$ is $> 70\%$. Over the whole feasible range, the change in the average $\%BEV_{ss}$ was only 10% as shown in Fig. 6 meaning that the BEV_{com} and TF_{thr} have a limited effect on the $\%BEV_{ss}$.

Repeating this scenario, but with $PHEV_{com}$ and $PHEV_{rt}$ fixed at 0.25 and 0.05 showed a similar curve to that in Fig. 5. The average difference in the monthly energy is 0.8 MWh between the two cases. Comparing this difference with the standard deviation of the results (0.57 MWh), then the two curves are undistinguishable, and therefore, this difference can be ignored. In other words, the $PHEV_{com}$ and $PHEV_{rt}$ have a limited impact on the relationship between the BEV_{com} and TF_{thr} and the monthly energy. This is also true for the $\%BEV_{ss}$ relationship with BEV_{com} and TF_{thr}.

3.1.2. $PHEV_{com}$, $PHEV_{rt}$ and $\%bev_{ss}$.

From Fig. 5, different operating points can provide the same amount of energy. Assuming an energy level of 15 MWh, a possible setting from Fig. 5 for the TF_{thr} and the BEV_{com} is 0.55 and 0.65, respectively (exact corresponding energy is 14.75 MWh). $PHEV_{com}$ and $PHEV_{rt}$ were changed between 0 and 0.5 while keeping the TF_{thr} and the BEV_{com} fixed at 0.55 and 0.65, respectively.

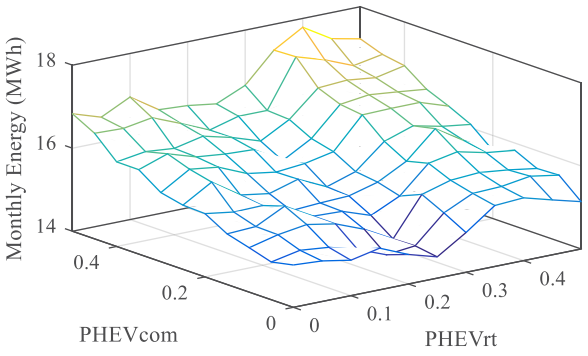

Fig. 7. Variation of $PHEV_{com}$ and $PHEV_{rt}$ with monthly energy demand.

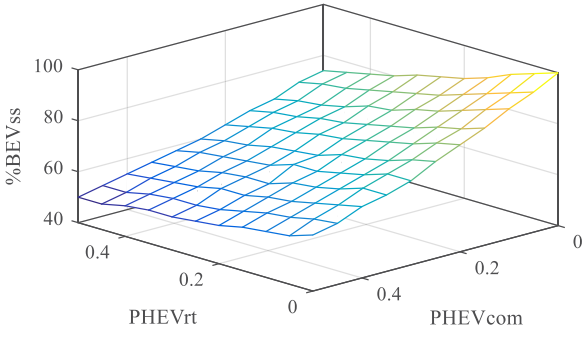

Fig. 8. Variation of $PHEV_{com}$ and $PHEV_{rt}$ with $\%BEV_{ss}$.

The average monthly energy and $\%BEV_{ss}$ are shown in Figs. 7 and 8, respectively. The average standard deviation is 0.64 MWh for the monthly energy and 1.6% for the $\%BEV_{ss}$. Lower $PHEV_{rt}$ values have less effect than higher $PHEV_{rt}$ values on the energy. Compared with the variation of BEV_{com} and TF_{thr}, it is clear that the BEV_{com} and TF_{thr} have the major impact on the monthly energy while the $PHEV_{com}$ and $PHEV_{rt}$ predominantly affects the $\%BEV_{ss}$. This conclusion does not eliminate any dependency between the parameters, though the result is stable with variation in BEV_{com} and TF_{thr}. Repeating this scenario, but with BEV_{com} and TF_{thr} fixed at 0.4 and 0.7 at the same energy level does not influence the relationship between the $\%BEV_{ss}$ and the $PHEV_{com}$ and $PHEV_{rt}$ (Fig. 8). Furthermore, changing the monthly energy by 20% showed a $<3\%$ ($\%BEV_{ss} > 70\%$) difference from that in Fig. 8.

3.1.3. $\%BEV_{ss}$ level and monthly energy, BEV_{com} and TF_{thr}

This case tests the effect of changing the $\%BEV_{ss}$ level, as defined by the $PHEV_{com}$ and $PHEV_{rt}$, on the relationship between

the monthly energy and the BEV_{com} and TF_{thr}. From Fig. 8, the $\%BEV_{ss}$ at $PHEV_{com}$ of 0.1 and $PHEV_{rt}$ of 0.25, used in the first scenario, is equal to 77%. Both the $PHEV_{com}$ and the $PHEV_{rt}$ were set to 0.1 corresponding to a $\%BEV_{ss}$ of 85% in Fig. 8. The average difference in the monthly energy between the first and third scenarios was only 0.33 MWh. The influence of changing the $\%BEV_{ss}$ level (8% change between the two scenarios) is small and will be ignored. Therefore, the same curve points can be used for representing the relationship between the monthly energy and the BEV_{com} and TF_{thr}.

3.1.4. Summary

From the previous three scenarios, we conclude:

- BEV_{com} and TF_{thr} are key in determining the monthly energy level (Figs. 5 and 7). Whilst $PHEV_{com}$ and $PHEV_{rt}$ affect more the $\%BEV_{ss}$ (Figs. 6 and 8).
- The relationship between the monthly energy and the BEV_{com} and TF_{thr} is little affected by changing the $\%BEV_{ss}$ level.
- A 20% change in the monthly energy causes a change of $<3\%$ in the relationship between $\%BEV_{ss}$ and the $PHEV_{com}$ and $PHEV_{rt}$ for $\%BEV_{ss} > 70\%$.
- For the same $\%BEV_{ss}$ as defined by the two parameters $PHEV_{com}$ and $PHEV_{rt}$, different settings for these two parameters do not affect the relationship between the $\%BEV_{ss}$ and the BEV_{com} and TF_{thr}.
- For the same energy level, different combinations for the BEV_{com} and TF_{thr} can be used. Changing the setting point does not affect the relationship between the $\%BEV_{ss}$ and the $PHEV_{com}$ and $PHEV_{rt}$.

Accordingly, the following five steps are the proposed guide for setting the four parameters:

1. Save the data in Figs. 5, 6, and 8 with energy values rounded to the nearest quarter as lookup tables.
2. For the required $\%BEV_{ss}$ that matches the nominal site utilization, pick all possible $PHEV_{com}$ and $PHEV_{rt}$ combinations that satisfy this $\%BEV_{ss}$.
3. Choose any setting for the $PHEV_{com}$ and $PHEV_{rt}$. Noting that high $PHEV_{rt}$ values are not recommended.
4. For the required energy demand, pick all possible BEV_{com} and TF_{thr} combinations that satisfy this demand.
5. For the possible combinations in step 4, find the corresponding $\%BEV_{ss}$ values (data saved from Fig. 6). Choose a setting for the BEV_{com} and TF_{thr} that provides a $\%BEV_{ss}$ close to the required value. If different combinations satisfy this point, then choose any setting.

As the data in Fig. 6 was derived for a $\%BEV_{ss}$ of 77% then the maximum value is 80%. Therefore, if the required $\%BEV_{ss}$ is $>$ 77%, step 5 in the previous procedure may be not achievable and it can be omitted.

3.2. Model output

The model has been executed using the values for different parameters e.g. the local fleet composition, distribution for plug-in time, and SoC distributions. For the competitive charging parameters, models will be unique if based on real operational data and specific local characteristics. The model has been tested at a monthly energy demand of 17 MWh, and a $\%BEV_{ss}$ of 80% and 85%.[1]

[1] Monthly data obtained from Gridserve, *priv. comm.*

Table 5
Possible settings for energy = 17 MWh and %BEVss = 80%.

$PHEV_{com}/PHEV_{rt}$	0/0.35	0.10/0.20	0.20/0.05	
BEV_{com}/TF_{thr}	0.40/0.80	0.55/0.75	0.70/0.65	0.80/0.55

Table 6
Model output for energy = 17 and %BEVss = 80%.

$PHEV_{com}/PHEV_{rt}$	BEV_{com}/TF_{thr}	Energy (MWh)		$\%BEV_{ss}$	
		Mean	Std	Mean	Std
0/0.35	0.40/0.80	17.8	0.63	76	1
	0.80/0.55	17.4	0.70	82	2
0.10/0.20	0.40/0.80	16.7	0.67	79	1
	0.80/0.55	16.8	0.80	81	1
0.20/0.05	0.40/0.80	17.1	0.55	81	1
	0.80/0.55	17.5	0.68	81	1

Table 7
Model output for energy = 17 MWh and %BEVss = 85%.

BEV_{com}/TF_{thr}	Energy (MWh)		$\%BEV_{ss}$	
	Mean	Std	Mean	Std
0.40/0.80	17.0	0.73	84	1
0.55/0.75	17.5	0.63	86	1
0.70/0.65	17.6	0.62	86	2
0.80/0.55	17.0	0.68	86	1

For a %BEVss of 80% and following the proposed procedure to set the competitive charging parameters, three possible settings for the PHEVcom and PHEVrt and four different settings for the BEVcom and TFthr were found (Table 5). The model was run for the three possible settings for the PHEVcom and PHEVrt and the two extreme settings for the BEVcom and TFthr to show how changing the parameters affects the model output. For each setting group, the model has been executed for a month with 15 runs for each day.

Table 6 illustrates the average and standard deviation values for the energy and $\%BEV_{ss}$ for the six test cases. Despite the data used to extract the parameters setting corresponds to $\%BEV_{ss}$ of 77% (Fig. 5) and energy level of 15 MWh (Fig. 8), the model output for energy level of 17 MWh and $\%BEV_{ss}$ of 80% are close to the desired values.

For a $\%BEV_{ss}$ of 85% and demand of 17 MWh, the possible settings for BEV_{com} and TF_{thr} are given in Table 5. There are two possible combinations for ($PHEV_{com}$, $PHEV_{rt}$) as (0, 0.25) and (0.1, 0.1). Setting the $PHEV_{com}$ and $PHEV_{rt}$ to 0.1 and running the code for the four possible BEV_{com} and TF_{thr} settings, the output is given in Table 7. Similar to the previous test, the obtained energy and $\%BEV_{ss}$ are close to the desired values. It is worth noting that the maximum $\%BEV_{ss}$ in Fig. 6 is 80%. Therefore, none of the BEV_{com} and TF_{thr} settings in Table 5 correspond to 85%. However, the $\%BEV_{ss}$ obtained is close to the desired value ensuring that the BEV_{com} and the TF_{thr} do not have undue influence on the $\%BEV_{ss}$.

To illustrate the range of outputs, the EV arrival distribution for an iteration for one day is shown in Fig. 9 for the local and passing traffic populations. The corresponding charging power is shown in Fig. 10. The daily required charging energy over the whole month is given in Fig. 11. Finally, Figs. 12 and 13 show the distribution of the total monthly EV arrival from the two populations. The average arrival (15 iterations) at each time slot is shown together with the error bars representing the standard deviation. The monthly EV arrival matches the modelled plug-in time distribution and the traffic flow distribution for the local and passing traffic populations, respectively.

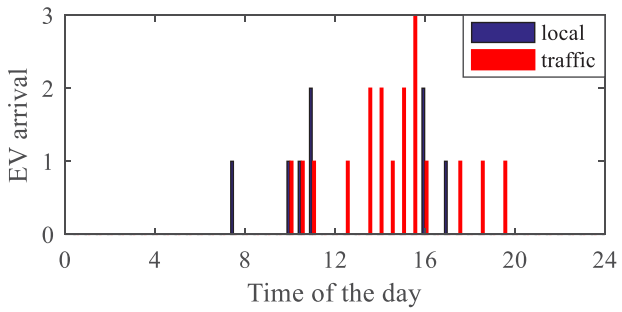

Fig. 9. EV arrival distribution for one day.

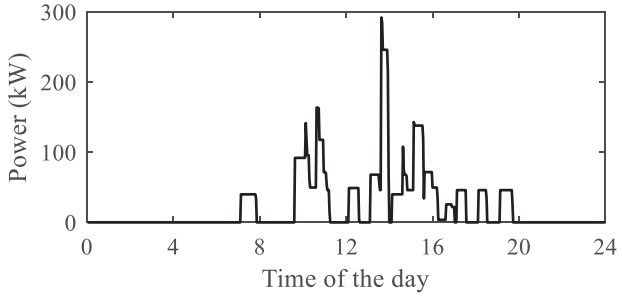

Fig. 10. Charging power for a typical day.

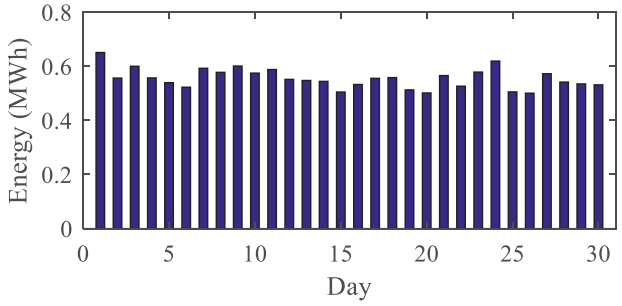

Fig. 11. Daily charging energy for a whole month.

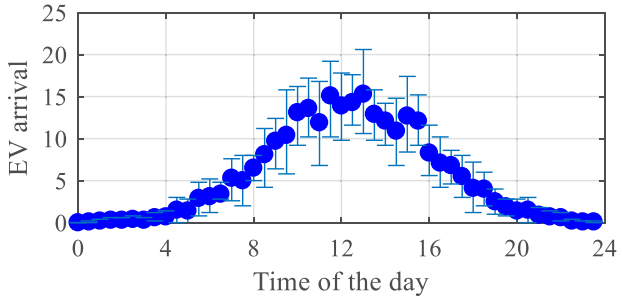

Fig. 12. Monthly EV arrival distribution from the local population.

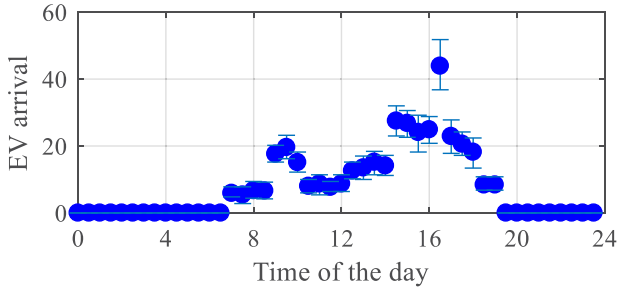

Fig. 13. Monthly EV arrival distribution from the passing traffic.

4. Conclusions and further work

The growth of EVs is slowed by a lack of easy to use and reliable charging infrastructure, especially rapid charging facilities with an experience similar to conventional refuelling stations. Such stations will likely be used mainly by BEVs rather than PHEVs because large capacity batteries require charging rates higher than can be accommodated by at-home on on-street facilities.

Designing and operating a large multi-charger station depends on an optimization process of parameters such as arrival rate and the technical specifications of different EV types. The parameters characterizing whether an EV needs to charge are shaped by the habits of drivers, thus in their nature are stochastic and not deterministic. A stochastic model for EV arrival has been developed to consider different uncertainties associated with daily travelled distance, vehicle battery SoC, start time of charging events, and vehicle parameters. In this way, the model can mimic observable power demand for a charging facility resulting from patterns in EV owner/driver behaviour and travel patterns. The model uniquely treats EVs as local and passing traffic populations, plus separating BEVs and PHEVs. The steps for estimating arrival rates from each population were discussed in detail, accounting for seasonality. The model incorporates competitive charging between the forecourt and other facilities. Sensitivity of the model to different parameters controlling the competitive charging was investigated, resulting in a procedure to better understand and set these parameters. The model addresses the gap in knowledge between a detailed physics-based power systems and power electronics model of the charging process, and a purely behavioural or economics view of EV fleet characteristics.

By using the UK's first dedicated large-scale multi-charger forecourt as a case study, the model was tested and validated with real-world data. The model was able to produce plausible EV arrival patterns for both of the population types, and reproduce the characteristic power demand at the site. All estimates incorporate uncertainty, reflecting the realistic variability of the parameters of interest. Together, these allow the site operator to plan daily activities, interact with the local grid operator, and to inform investment decisions. The model in independent of location, uses open-source data, and is structured flexibly, making it is relatively straightforward to adapt to any potential site as part of the technical and business planning process.

Future development will be directed to using real operational data for predicting daily demand, applying this model to other types of location e.g. city centre, and understanding how projected growth of EV use will affect the requirements for charging infrastructure and impact the electrical power distribution grid.

CRediT authorship contribution statement

F.M. Aboshady: Formal analysis, Investigation, Writing – original draft. **I. Pisica:** Funding acquisition, Methodology, Writing - review & editing. **C.J. Axon:** Funding acquisition, Project administration, Supervision, Conceptualization, Methodology, Writing – review & editing.

Declaration of competing interest

The authors declare that they have no known competing financial interests or personal relationships that could have appeared to influence the work reported in this paper.

Data availability

Data will be made available on request.

Acknowledgements

This work was supported by the UK Research Council (UKRI) through Innovate UK under grant No. TS/T006471/1. We thank the consortium partners GRIDSERVE,Upside Energy, and Essex County Council for constructive feedback on this work.

Appendix. Algorithms for estimating ev arrival from the local population

Algorithm I.

Start of the day.
$N_{ev} = 0$.
FOR k = 1 : local fleet size
  Pick a random distance from the daily travelled distance distribution
  Add the daily distance to the accumulated distance since last charging
  Estimate the likely current SoC for this EV using (1)
  IF current SoC < Threshold SoC
    $N_{ev} = N_{ev} + 1$
    Record this EV parameters
  ENDIF
ENDFOR
OUTPUT N_{ev} and the corresponding EVs parameters

Algorithm II.

INPUT N_{ev} from the first step
FOR k = 1 : 48
  Slot upper limit SUL = N_{ev} – Σ EV arrival during previous slots
  Generate an integer random number N between 0 and SUL
  Generate N random values between 0 and 1
  Threshold value = Plug-in time likelihood at this time of the day
  Slot arrival = 0
  FOR m = 1 : N
    IF random value (m) <= Threshold value
      Slot arrival = Slot arrival + 1
    ENDIF
  ENDFOR
  SAVE EV arrival for the current time slot
ENDFOR
OUTPUT EV arrival at each of the 48 time slots

References

Aboshady, F.M., Pisica, I., Axon, C.J., 2021. Stochastic modeling of vehicle arrival for the UK's first electric vehicle charging forecourt. In: 2021 IEEE Power & Energy Society Innovative Smart Grid Technologies Conference. ISGT, pp. 1–5.

Ahmad, F., Iqbal, A., Ashraf, I., Marzband, M., Khan, I., 2022. Optimal location of electric vehicle charging station and its impact on distribution network: A review. Energy Rep. 8, 2314–2333.

Almutairi, A., Alyami, S., 2021. Load profile modeling of plug-in electric vehicles: Realistic and ready-to-use benchmark test data. IEEE Access 9, 59637–59648.

Bharathidasan, M., Indragandhi, V., Suresh, V., JasiŃSki, M., Leonowicz, Z., 2022. A review on electric vehicle: Technologies, energy trading, and cyber security. Energy Rep. 8, 9662–9685.

Birk Jones, C., Vining, W., Lave, M., Haines, T., Neuman, C., Bennett, J., Scoffield, D.R., 2022. Impact of electric vehicle customer response to time-of-use rates on distribution power grids. Energy Rep. 8, 8225–8235.

Brady, J., O'Mahony, M., 2016. Modelling charging profiles of electric vehicles based on real-world electric vehicle charging data. Sustainable Cities Soc. 26, 203–216.

Buzna, L., De Falco, P., Ferruzzi, G., Khormali, S., Proto, D., Refa, N., Straka, M., Van Der Poel, G., 2021. An ensemble methodology for hierarchical probabilistic electric vehicle load forecasting at regular charging stations. Appl. Energy 283, 116337.

Cheng, J., Xu, J., Chen, W., Song, B., 2022. Locating and sizing method of electric vehicle charging station based on Improved Whale Optimization Algorithm. Energy Rep. 8, 4386–4400.

Daina, N., Sivakumar, A., Polak, J.W., 2017. Modelling electric vehicles use: a survey on the methods. Renew. Sustain. Energy Rev. 68, 447–460.

Deng, Q., Tripathy, S., Tylavsky, D., Stowers, T., Loehr, J., 2018. Demand modeling of a dc fast charging station. In: 2018 North American Power Symposium. NAPS, Fargo, ND, USA.

Department for Transport, 2017. Statistics and data about the National Travel Survey. [Online]. Available: https://www.gov.uk/government/collections/national-travel-survey-statistics [Accessed 6/8/2020].

Department for Transport, 2019. Road traffic statistics. [Online]. Available: https://roadtraffic.dft.gov.uk [Accessed 20/5/2021].

Department for Transport, 2020a. Experimental statistics on observed charging patterns for local authority rapid chargepoints in England in 2017. [Online]. Available: https://www.gov.uk/government/statistics/electric-chargepoint-analysis-2017-local-authority-rapids [Accessed 20/5/2021].

Department for Transport, 2020b. Statistics and data about the number of licensed vehicles. [Online]. Available: https://www.gov.uk/government/collections/vehicles-statistics [Accessed 9/6/2021].

Dixon, J., Elders, I., Bell, K., 2018. Characterization of electric vehicle fast charging forecourt demand. In: 2018 IEEE PES Innovative Smart Grid Technologies Conference Europe (ISGT-Europe). Sarajevo, Bosnia and Herzegovina.

Duan, P., Askari, M., Hemat, K., Ali, Z.M., 2021. Optimal operation and simultaneous analysis of the electric transport systems and distributed energy resources in the smart city. Stain. Cities Soc. 75, 103306.

Elghitani, F., El-Saadany, E.F., 2021. Efficient assignment of electric vehicles to charging stations. IEEE Trans. Smart Grid 12, 761–773.

EV Database, 2020. Electric vehicle database. [Online]. Available: https://ev-database.uk [Accessed 20/5/2021].

Goel, S., Sharma, R., Rathore, A.K., 2021. A review on barrier and challenges of electric vehicle in India and vehicle to grid optimisation. Transp. Eng. 4.

Harris, C.B., Webber, M.E., 2014. An empirically-validated methodology to simulate electricity demand for electric vehicle charging. Appl. Energy 126, 172–181.

Hill, G., Heidrich, O., Creutzig, F., Blythe, P., 2019. The role of electric vehicles in near-term mitigation pathways and achieving the UK's carbon budget. Appl. Energy 251.

Humayd, A.S.B., Bhattacharya, K., 2018. A novel framework for evaluating maximum PEV penetration into distribution systems. IEEE Trans. Smart Grid 9, 2741–2751.

Huo, Y., Bouffard, F., Joós, G., 2017. An energy management approach for electric vehicle fast charging station. In: 2017 IEEE Electrical Power and Energy Conference. EPEC, Saskatoon, SK, Canada.

Kavianipour, M., Fakhrmoosavi, F., Singh, H., Ghamami, M., Zockaie, A., Ouyang, Y., Jackson, R., 2021. Electric vehicle fast charging infrastructure planning in urban networks considering daily travel and charging behavior. Transp. Res. Part Transp. Environ. 93, 102769.

Korolko, N., Sahinoglu, Z., Nikovski, D., 2016. Modeling and forecasting self-similar power load due to EV fast chargers. IEEE Trans. Smart Grid 7, 1620–1629.

Moon, H., Park, S.Y., Jeong, C., Lee, J., 2018. Forecasting electricity demand of electric vehicles by analyzing consumers' charging patterns. Transp. Res. Part D 62, 64–79.

Moradipari, A., Tucker, N., Alizadeh, M., 2021. Mobility-aware electric vehicle fast charging load models with geographical price variations. IEEE Trans. Transp. Electrif. 7, 554–565.

Morrissey, P., Weldon, P., O'Mahony, M., 2016. Future standard and fast charging infrastructure planning: An analysis of electric vehicle charging behaviour. Energy Policy 89, 257–270.

Pan, L., Yao, E., Yang, Y., Zhang, R., 2020. A location model for electric vehicle (EV) public charging stations based on drivers' existing activities. Sustain. Cities Soc. 59, 102192.

Powell, S., Cezar, G.V., Rajagopal, R., 2022. Scalable probabilistic estimates of electric vehicle charging given observed driver behavior. Appl. Energy 309, 118382.

Qian, K., Zhou, C., Allan, M., Yuan, Y., 2011. Modeling of load demand due to EV battery charging in distribution systems. IEEE Trans. Power Syst. 26, 802–810.

Robinson, A.P., Blythe, P.T., Bell, M.C., HÜBner, Y., Hill, G.A., 2013. Analysis of electric vehicle driver recharging demand profiles and subsequent impacts on the carbon content of electric vehicle trips. Energy Policy 61, 337–348.
Sadhukhan, A., Ahmad, M.S., Sivasubramani, S., 2021. Optimal allocation of EV charging stations in a radial distribution network using probabilistic load modeling. IEEE Trans. Intell. Transp. Syst. 1–10.
Schäuble, J., Kaschub, T., Ensslen, A., Jochem, P., Fichtner, W., 2017. Generating electric vehicle load profiles from empirical data of three EV fleets in Southwest Germany. J. Cleaner Prod. 150, 253–266.
Shepero, M., Munkhammar, J., Widén, J., Bishop, J.D.K., Boström, T., 2018. Modeling of photovoltaic power generation and electric vehicles charging on city-scale: A review. Renew. Sustain. Energy Rev. 89, 61–71.
Steen, D., Tuan, L.A., Carlson, O., Bertling, L., 2012. Assessment of electric vehicle charging scenarios based on demographical data. IEEE Trans. Smart Grid 3, 1457–1468.
Su, J., Lie, T.T., Zamora, R., 2019. Modelling of large-scale electric vehicles charging demand: A New Zealand case study. Electr. Power Syst. Res. 167, 171–182.
Tang, D., Wang, P., 2016. Probabilistic modeling of nodal charging demand based on spatial–temporal dynamics of moving electric vehicles. IEEE Trans. Smart Grid 7, 627–636.
Tehrani, N.H., Wang, P., 2015. Probabilistic estimation of plug-in electric vehicles charging load profile. Electr. Power Syst. Res. 124, 133–143.
Uimonen, S., Lehtonen, M., 2020. Simulation of electric vehicle charging stations load profiles in office buildings based on occupancy data. Energies (13).
Ul-Haq, A., Cecati, C., El-Saadany, E., 2018. Probabilistic modeling of electric vehicle charging pattern in a residential distribution network. Electr. Power Syst. Res. 157, 126–133.
Yan, Q., Lin, H., Li, J., Ai, X., Shi, M., Zhang, M., Gejirifu, D., 2022. Many-objective charging optimization for electric vehicles considering demand response and multi-uncertainties based on Markov chain and information gap decision theory. Sustain. Cities Soc. 78, 103652.
Yi, Z., Bauer, P.H., 2016. Spatiotemporal energy demand models for electric vehicles. IEEE Trans. Veh. Technol. 65, 1030–1042.
Zap-MAP, 2021. EV charging stats 2021. [Online]. Available: https://www.zap-map.com/statistics/ [Accessed 10/5/2021].
Zhang, H., Sheppard, C.J.R., Lipman, T.E., Zeng, T., Moura, S.J., 2020. Charging infrastructure demands of shared-use autonomous electric vehicles in urban areas. Transp. Res. Part Transp. Environ. 78, 102210.
Zheng, Y., Shao, Z., Zhang, Y., Jian, L., 2020. A systematic methodology for mid-and-long term electric vehicle charging load forecasting: The case study of Shenzhen, China. Sustainable Cities Soc. 56.
Zhu, J., Yang, Z., Guo, Y., Zhang, J., Yang, H., 2019a. Short-term load forecasting for electric vehicle charging stations based on deep learning approaches. Appl. Sci. 9.
Zhu, J., Yang, Z., Mourshed, M., Guo, Y., Zhou, Y., Chang, Y., Wei, Y., Feng, S., 2019b. Electric vehicle charging load forecasting: A comparative study of deep learning approaches. Energies 12.